SRNL-STI-2009-00084, REVISION 0

Key Words:
DWPF, noble metals
Hydrogen, SRAT

Retention:
Permanent

STATISTICAL EVALUATION OF PROCESSING DATA FROM THE RH-RU-HG MATRIX STUDY

D. C. Koopman

APRIL 2009

Savannah River National Laboratory
Savannah River Nuclear Solutions
Aiken, SC 29808

Prepared for the U.S. Department of Energy Under
Contract Number DE-AC09-08SR22470

SRNL
SAVANNAH RIVER NATIONAL LABORATORY

DISCLAIMER

Printed in the United States of America

Prepared for
U.S. Department of Energy

Key Words:
DWPF, noble metals
Hydrogen, SRAT

Retention:
Permanent

STATISTICAL EVALUATION OF PROCESSING DATA FROM THE RH-RU-HG MATRIX STUDY

D. C. Koopman

APRIL 2009

Savannah River National Laboratory
Savannah River Nuclear Solutions
Savannah River Site
Aiken, SC 29808

Prepared for the U.S. Department of Energy Under
Contract Number DE-AC09-08SR22470

SRNL
SAVANNAH RIVER NATIONAL LABORATORY

REVIEWS AND APPROVALS

D. C. Koopman, Process Engineering Technology Date

T. B. Edwards, Peer Reviewer, Statistical Consulting Date

M. E. Stone, Peer Reviewer, Process Engineering Technology Date

C. C. Herman, Manager, Process Engineering Technology Date

S. L. Marra, Manager Date
Environmental & Chemical Process Technology Research Programs

J. E. Occhipinti, Manager Date
Waste Solidification Engineering

TABLE OF CONTENTS

LIST OF FIGURES

LIST OF TABLES

LIST OF ACRONYMS

ACTL	Aiken County Technology Laboratory
AD	Analytical Development
ASP	Analytical Study Plan
CPC	Chemical Process Cell
DWPF	Defense Waste Processing Facility
E&CPT	Environmental and Chemical Process Technology
FAVC	Formic Acid Vent Condenser
GC	Gas Chromatograph
IC	Ion Chromatography
ICP-AES	Inductively Coupled Plasma-Atomic Emission Spectroscopy
JMP	Statistical software package used during analysis
LWO	Liquid Waste Organization
MWWT	Mercury Water Wash Tank
PSAL	Process Science Analytical Laboratory
QA	Quality Assurance
SME	Slurry Mix Evaporator
SRAT	Sludge Receipt and Adjustment Tank
SRNL	Savannah River National Laboratory
SRNS	Savannah River Nuclear Solutions, LLC
TA	Technical Analyst
TIC	Total Inorganic Carbon
TR	Technical Report
TT&QAP	Task Technical and Quality Assurance Plan
TTR	Task Technical Request
WSRC	Washington Savannah River Company
XAS	X-ray Absorption Spectroscopy

1.0 EXECUTIVE SUMMARY

An evaluation of the statistical significance of Rh, Ru, and Hg on DWPF Sludge Receipt and Adjustment Tank (SRAT) cycle catalytic hydrogen generation and process chemistry was conducted by the Savannah River National Laboratory (SRNL) using a full-factorial experimental design. This test design can identify significant interactions between these three species in addition to individual effects. Statistical modeling of data from the Rh-Ru-Hg matrix study has been completed. Preliminary data and conclusions were given in an earlier report.[10] This final report concludes the work on the Rh-Ru-Hg matrix study. Modeling results are summarized below.

Rhodium was found to:

- Promote increased total hydrogen mass.
- Promote an increase in the maximum hydrogen generation rate.
- Promote an increase in the hydrogen generation rate shortly after acid addition.
- Shorten the elapsed time between acid addition and the maximum hydrogen generation rate.
- Increase formate loss.
- Inhibit NO_2 and total NO_x off-gas species formation.
- Reduce nitrite-to-nitrate conversion.

Ruthenium was found to:

- Promote increased total hydrogen mass.
- Promote an increase in the maximum hydrogen generation rate.
- Promote an increase in the hydrogen generation rate in the second half of the SRAT cycle.
- Promote an increase in total CO_2 generated.
- Increase formate loss.
- Promote NO_2 and total NO_x off-gas species formation.
- Reduce nitrite-to-nitrate conversion.

Mercury was found to:

- Inhibit total hydrogen mass produced.
- Promote an increase in total CO_2 generated.
- Promote NO_2 off-gas species formation.
- Inhibit total NO_x off-gas species formation.

Results confirmed qualitative observations that Rh was activating before Ru for hydrogen generation. An interaction between Rh and Ru was present in the model for the total hydrogen generated during the SRAT, perhaps because the total combined contributions from two separate episodes of hydrogen generation. The first episode was dominated by Rh and

the second by Ru. Consequently, the linear statistical model was asked to explain more than one phenomenon and included more terms.

Mercury did not significantly impact hydrogen generated by either Rh or Ru in models in this study (all tests had Hg ≥ 0.5 wt% in total solids), whereas tests in Sludge Batches 3 and 4 (SB3 and SB4) with and without Hg showed a very significant negative impact from adding Hg. The conclusion is that once a small quantity of Hg is present, the primary inhibiting effect of Hg is in place, and hydrogen generation is relatively insensitive to further increases in total Hg. Any secondary Hg effects were difficult to quantify and model. Mercury was found to be statistically significant, however, as an inhibiting factor for hydrogen generation when modeling was based on the logarithm of the hydrogen generation rate.

Only limited statistical evidence was found for non-linearity and quadratic dependence of other SRAT process measures, such as formate loss or total NO_x generation, on the three matrix variables. The interaction term for Ru with Hg, however, appeared in models for total CO_2, total NO_2, and total moles of nitrogen-derived off-gas species. A single interaction between Ru and Hg during nitrite destruction could explain all three of these effects in the observed responses. Catalytic decomposition of nitrite ion by formic acid produces CO_2 plus either NO or N_2O. The vast majority of the NO produced is converted to NO_2, and NO_2 is the major fraction of the total moles of nitrogen in the off-gas species.

Future experimental work related to catalytic hydrogen generation control is expected with regard to minimizing formic acid use through alternative reductants as well as in pursuing mesoporous media for sequestering the catalytically active noble metals to inhibit catalytic hydrogen generation. Two alternative stoichiometric acid equations are also under development. A summary document is in draft form that provides an overview of progress made in understanding catalytic hydrogen generation as well as the progress made in resolving open issues from the one external and two internal reviews of the catalytic hydrogen generation program.

2.0 INTRODUCTION

Due to greater than expected hydrogen generation during the Tank 51-Sludge Batch 4 (SB4) qualification run, SC-0, DWPF Engineering requested that the Savannah River National Laboratory (SRNL) expand the on-going catalytic hydrogen generation program designed to increase the understanding of catalytic chemistry in the DWPF Sludge Receipt and Adjustment Tank and Slurry Mix Evaporator (SRAT and SME, respectively).

The work presented in this technical report was identified as a result of SRNL/Liquid Waste Organization (LWO) meetings to define potential causes of catalytic hydrogen generation as well as from an external technical review panel commissioned to evaluate SRNL hydrogen related data and programs.[1] The work scope was covered under the technical task request: HLW-DWPF-TTR-2007-0016.[2] A task technical and quality assurance plan (TT&QAP[3]) was drafted to address the needs of the TTR which included issues that were raised in meetings with LWO plus some of the recommendations made by the review panel. A supporting analytical study plan was issued.[4]

The testing discussed in this report focuses on the effects of Rh, Ru, and Hg in a single system with other important variables held constant. The need for this testing became apparent following completion of earlier parts of the hydrogen program. 'Impact of mercury' studies on hydrogen generation in the SB3 system were the first to indicate a potential need for follow-up work.[5] The 2005 form of noble metal tests showed a correlation between soluble Rh and Ru with hydrogen generation which helped to narrow the planned test scope.[6, 7] These earlier results, along with additional data obtained during SB4 testing,[8] set the scope of this study as the statistical evaluation of the significance of main factor and two-way interaction effects due to Rh, Ru, and Hg on hydrogen generation. In particular, it was desired to gain a better understanding of the significance of Hg interactions with the noble metal catalysts to inhibit hydrogen generation for typical site waste compositions.

Simulant preparation and preliminary flowsheet studies have been documented.[9] Experimental results from twelve initial Rh-Ru-Hg process simulations have also been documented.[10] Ag and Pd were fixed at 0.003 and 0.001 wt% of total solids, respectively, in the Rh-Ru-Hg matrix testing. Rh, Ru, and Hg were varied from 1/3 to 5/3 of the preliminary flowsheet study values (0.0078, 0.030, and 1.50 wt% of total solids respectively). The Rh and Ru ranges cover measured concentrations of these two noble metals in Sludge Batches 1B through 5. The mercury range was not extended to include zero, although sludge batches 1A and 3 had less than 0.5 wt% initial Hg. The DWPF SRAT product maximum Hg content is specified as 0.45 wt% Hg in the total solids. The range of initial Hg values from 0.5-2.5 wt% in the total solids was chosen to cover an interesting portion of the likely range of DWPF feeds while avoiding anomalous behavior near zero Hg.

The Rh-Ru-Hg matrix testing did not require hydrogen generation above the scaled equivalent of the 0.65 lbs H_2/hr from the DWPF design basis for the SRAT. It was anticipated, however, that hydrogen generation rates could approach the DWPF limit when

Rh and/or Ru were at their maximum values based on the data from the preliminary flowsheet tests at the midpoint concentrations.

Prior statistical work found correlations between Rh and hydrogen.[11] These were effectively correlations between hydrogen and all noble metals simultaneously. The individual noble metal concentrations were highly correlated by their fission yield ratios, and the statistical models could not meaningfully distinguish the effects of one noble metal from the effects of another. Mercury interaction effects were also found to be statistically significant in some previous statistical models, whether interacting with noble metals or with various measures of added acid. A statistically significant effect of mercury by itself, however, on the SRAT maximum hydrogen generation rate was not detected in the prior work. Nitrite ion, as well as SRAT product nitrate which can reflect nitrite-to-nitrate conversion, also appeared in some of the statistical models for hydrogen generation.

The simulations listed in Table 1 constitute a full-factorial experimental design on three factors at two levels plus a midpoint. The position column indicates whether the factors Rh, Ru, and Hg respectively were at low (L), high (H), or midpoint (M) levels. This design supports testing for main (single factor) effects as well as for pair-wise and three-way interactions and for non-linearity. Three replicate runs were recommended for inclusion into the statistical design, at least one of which had to be the midpoint test. The initial plan had two replicates of non-midpoint tests as part of a twelve run matrix.

The matrix layout shifted slightly when data from two of the initial tests were rejected because of significant corrosion of the agitator shafts (RhRuHg2 and RhRuHg4). Corrosion reactions consumed acid and produced hydrogen making these two runs different from the others. Two replacement runs, RhRuHg14 and RhRuHg15, were performed to maintain the twelve run matrix. The final matrix had two replicates of the RhRuHg9 midpoint test (RhRuHg11 and RhRuHg15) and one replicate of a non-midpoint test. RhRuHg14 replaced one corroded shaft run, RhRuHg4, in the full factorial design test matrix. The other corroding shaft run, RhRuHg2, was replaced with RhRuHg12 (originally a replicate).

The purpose of the replicates was to quantify variability in the data that was not due to changing the concentrations of the three matrix factors. It was not critical that any particular non-midpoint tests be duplicated. There were some potential issues with the midpoint results in the original matrix, and consequently an additional replicate of the midpoint was substituted for a replicate of RhRuHg12 (to replace RhRuHg2).

Table 1 summarizes the fourteen SRAT cycles that were completed and the Rh, Ru, and Hg concentrations that were targeted. The runs are numbered RhRuHg1-2, 4-15. (RhRuHg3 was aborted early in the SRAT cycle due to equipment issues.) The final test block of twelve runs included RhRuHg1 and RhRuHg5-15, since RhRuHg2 and 4 were dropped because of chemistry associated with shaft corrosion. The final block of twelve SRAT cycles formed the basis for the statistical modeling work on the impacts of Rh, Ru, and Hg on processing.

Table 1. Test Matrix for Simulations

Run	Position	Rh, wt%§	Ru, wt%§	Hg, wt%§
RhRuHg1	L-L-L	0.00263	0.01012	0.506
RhRuHg2†	H-L-L	0.01315	0.01012	0.506
RhRuHg12 (replace 2)	H-L-L	0.01315	0.01012	0.506
RhRuHg10	L-H-L	0.00263	0.05056	0.505
RhRuHg4†	H-H-L	0.01314	0.05054	0.505
RhRuHg14 (replace 4)	H-H-L	0.01314	0.05054	0.505
RhRuHg5	L-L-H	0.00257	0.00990	2.475
RhRuHg6	H-L-H	0.01287	0.00990	2.474
RhRuHg13 (replicate)	H-L-H	0.01287	0.00990	2.474
RhRuHg7	L-H-H	0.00257	0.04948	2.472
RhRuHg8	H-H-H	0.01285	0.04946	2.472
RhRuHg9	M-M-M	0.00780	0.03000	1.500
RhRuHg11 (replicate)	M-M-M	0.00780	0.03000	1.500
RhRuHg15 (replicate)	M-M-M	0.00780	0.03000	1.500

† - Tests with a corroding agitator shaft (removed from final matrix analysis).
§ - Weight percent measured relative to total solids.

Additional details about the sludge simulant, acid stoichiometry, experimental conditions, sampling, analytical methods, and process data analysis are given in the preliminary report and not repeated here.[10] The two new SRAT runs followed the protocols outlined in the preliminary report. Neither run included a SME cycle. All data collected during the Rh-Ru-Hg matrix study that could be used to relate the SME cycle hydrogen generation rates to the processing conditions and SRAT cycle hydrogen generation rates were given in the preliminary report.

3.0 DISCUSSION OF EXPERIMENTAL DATA

This section presents the new experimental data from the two SRAT runs that were performed to replace data from tests with corroded agitator shafts. One of the new runs was also expected to help understand issues associated with the variability of the matrix midpoint tests. The two new runs were performed after the preliminary report was written.[10] Consequently, these data have not been previously documented.

3.1 SRAT RUN "RHRUHG14"

RhRuHg14 replaced RhRuHg4 (corroded shaft) in the final statistical test matrix. This factor combination was a particularly critical case to the planned statistical analysis, since it combined the maximum concentrations of Rh and Ru with the minimum concentration of the suspected inhibiting factor, Hg. Figure 1 compares RhRuHg14 data for hydrogen generation with data from two prior runs at high Rh and high Ru (two levels of Hg).

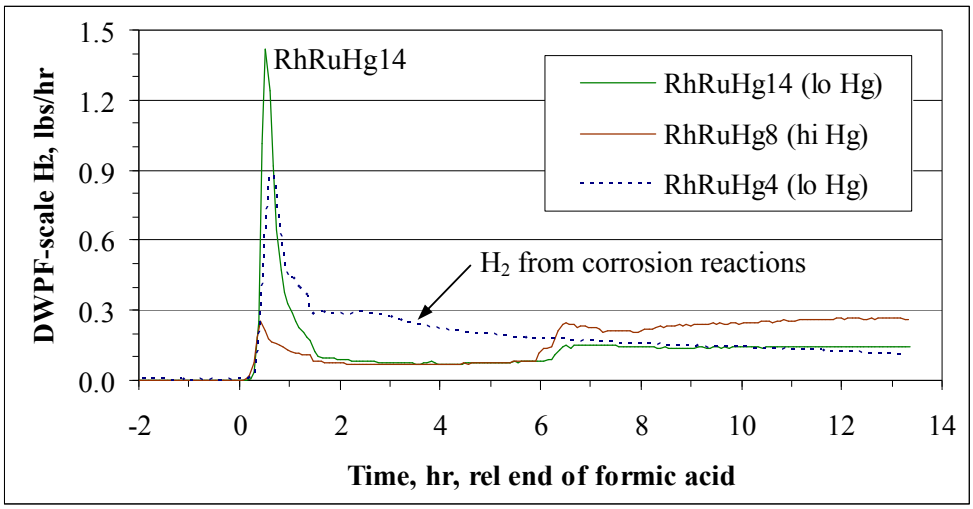

Figure 1. Impact of Hg on H_2 at high Rh-high Ru

Although RhRuHg4 data suggested that H_2 was generated from corrosion reactions (especially obvious from 1-6 hours after acid addition), the same quantity of acid in the absence of corrosion reactions led to a 46% higher maximum generation rate in RhRuHg14. The approximate matching of the hydrogen generation rates for high Hg case, RhRuHg8, and the low Hg case, RhRuHg14, after the initial peak (from 2-6 hours), followed by a period where the high mercury run generated hydrogen at a higher rate than the low mercury run, was seen in other test pairs. It is possible that the loss of excess acid from corrosion reactions by the time of the maximum hydrogen generation rate was more significant in reducing hydrogen production in RhRuHg4 than the corrosion reaction was in producing it (thus potentially explaining the lower peak rate in run 4 vs. 14). The RhRuHg14 hydrogen data are in better qualitative agreement with what was seen in the other matrix run data (early peak, drop to plateau, then a late increase about half-way through boiling).

Figure 2 and Figure 3 present the new data for carbon dioxide and nitrous oxide generation, respectively, compared to the prior data.

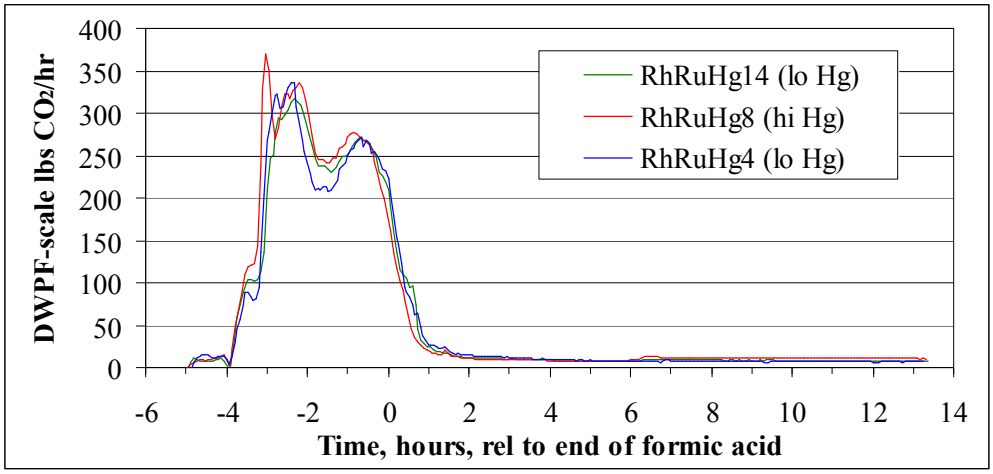

Figure 2. Impact of Hg on CO_2 at high Rh-high Ru

Variations in the carbon dioxide generation rate profiles were not very significant, which was not unexpected given the various mechanisms for CO_2 generation in the SRAT.

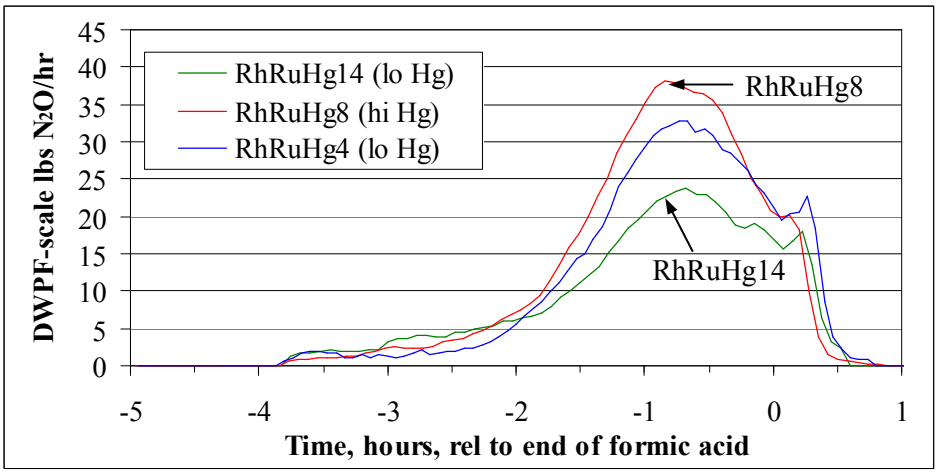

Figure 3. Impact of Hg on N_2O at high Rh-high Ru

There was a drop in N_2O production in RhRuHg14 relative to RhRuHg4. The statistical analysis in Section 4.3.3 failed to find a model that could explain the overall general variability in N_2O in terms of the three matrix variables. Acid consumed during shaft corrosion may be partly responsible for the data variability here.

The preliminary Rh-Ru-Hg matrix report presented comparisons of all hydrogen generation rate profiles at the high Rh concentration and all profiles at the high Ru concentration. These

included RhRuHg4. These graphs are reproduced below with RhRuHg14 data replacing RhRuHg4 data. Figure 4 compares all of the hydrogen generation rate data from the runs with high Rh (excluding RhRuHg4). On these figures, H = high, L = low, and the order is Rh-Ru-Hg, so H-L-H represents high Rh, low Ru, high Hg.

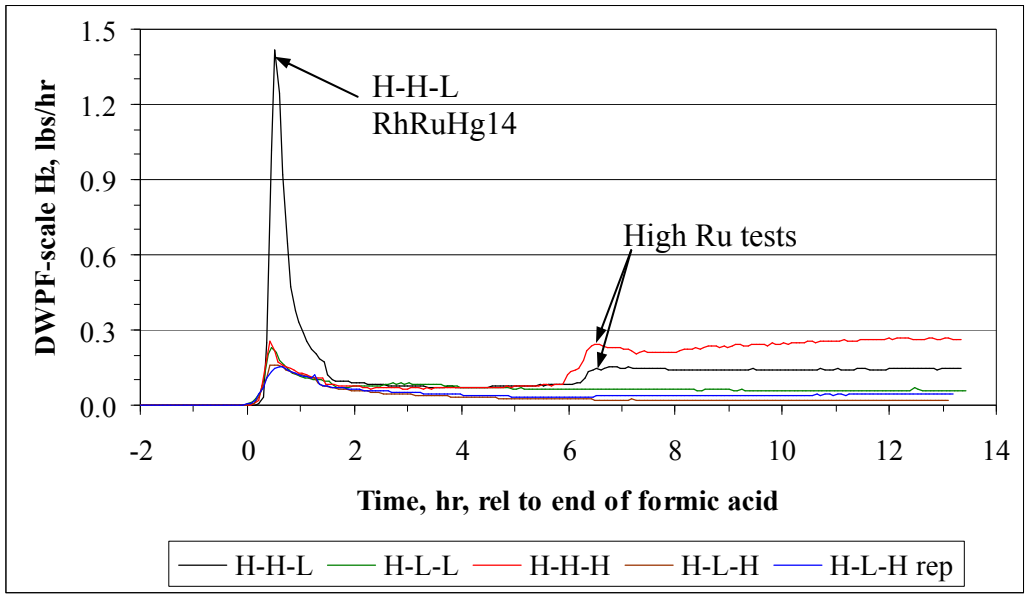

Figure 4. Hydrogen generation at high Rh loading

The two runs with high Ru produced more hydrogen from six hours after acid addition until the end of the SRAT cycle compared to the two cases (three runs) with low Ru.

Figure 5 presents the updated matrix hydrogen generation rate data for high Ru concentrations.

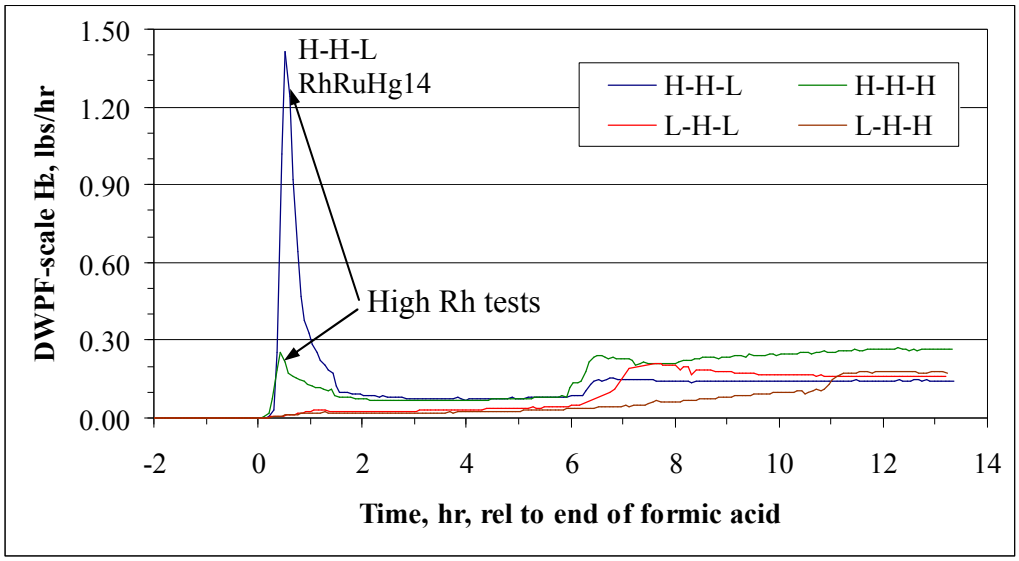

Figure 5. Hydrogen generation at high Ru loading

It is clear that the two high Rh runs produced much more hydrogen than the two low Rh runs in the first two hours after acid addition. All four runs experienced an increase in hydrogen generation rate during reflux. Three increases came about 6-7 hours after the end of acid addition, while the fourth came about 11 hours after the end of acid addition. The case that waited until 11 hours was the L-H-H case. The delay may have been driven by the low Rh-high Hg combination. Alternatively, the L-H-H run was one that used somewhat coarser HgO. It may be that the sequence of processing steps leading to stripping of the mercury was delayed by the initially larger size particles. This hypothesis is speculative, since no existing data would permit assessing the impact of HgO particle size on mercury chemical kinetics and processing. No other factors, however, were known to vary. (The low Ru cases did not experience a significant sudden increase in hydrogen generation during reflux, or at least not an increase that appeared to be a discrete event that occurred over a relatively small period of time. Such an effect may not have been quite so obvious with one-fifth the Ru loading.)

3.2 SRAT RUN "RHRUHG15"

The preliminary matrix results indicated a large difference between the two midpoint runs and a previous run, H2Sim4, with the same simulant, noble metal and mercury loading, and overall acid stoichiometry. A small difference in the fraction of total acid that was formic acid initially seemed insufficient to explain the observed differences. RhRuHg15 was another replicate of the matrix midpoint case. The hydrogen generation rates are compared in Figure 6.

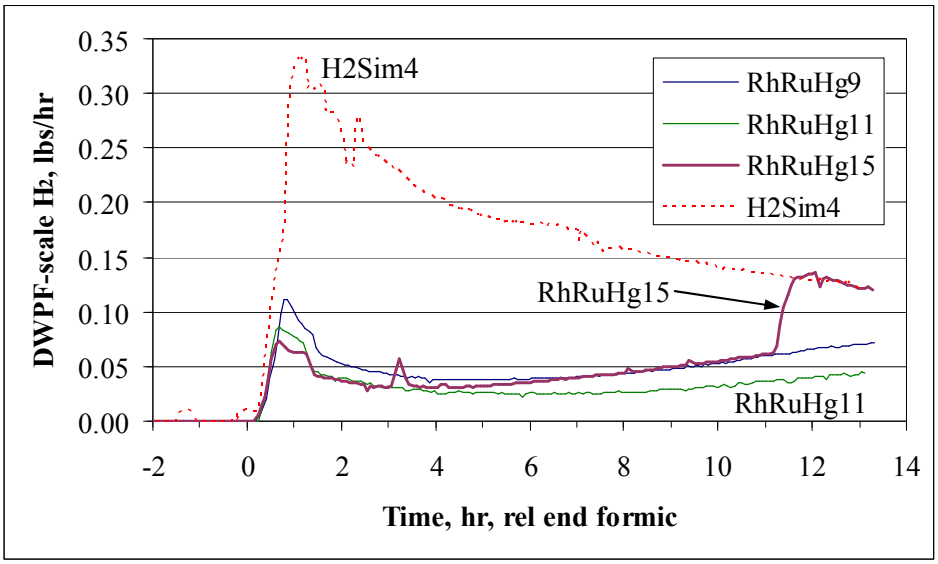

Figure 6. RhRuHg15 and other midpoint hydrogen data

The new midpoint run generally duplicated the features of the previous two matrix midpoint runs, RhRuHg9 and 11, during the first eleven hours after acid addition. The rapid increase in hydrogen generation between eleven and twelve hours after acid addition that brought the hydrogen generation rates up to the same curve that H2Sim4 had followed was unexpected. Apparently, the small variation in the fraction of acid that was formic acid (0.932 versus 0.913 in the matrix) did impact the H2Sim4 results significantly.

Sudden increases in catalytic activity for hydrogen generation during reflux were not uncommon in the matrix runs. Given that CO_2 generation exceeds H_2 generation by a significant amount, it remains a possibility that there are hydrogen consuming reactions that have not been identified which are sensitive to subtle changes in the processing. These reaction(s) may have been consuming more hydrogen during the matrix runs than during H2Sim4 for some undetermined reason.

Figure 7 presents the CO_2 generation rate data for the new midpoint run compared to the two prior matrix midpoint runs and the earlier preliminary flowsheet run, H2Sim4.

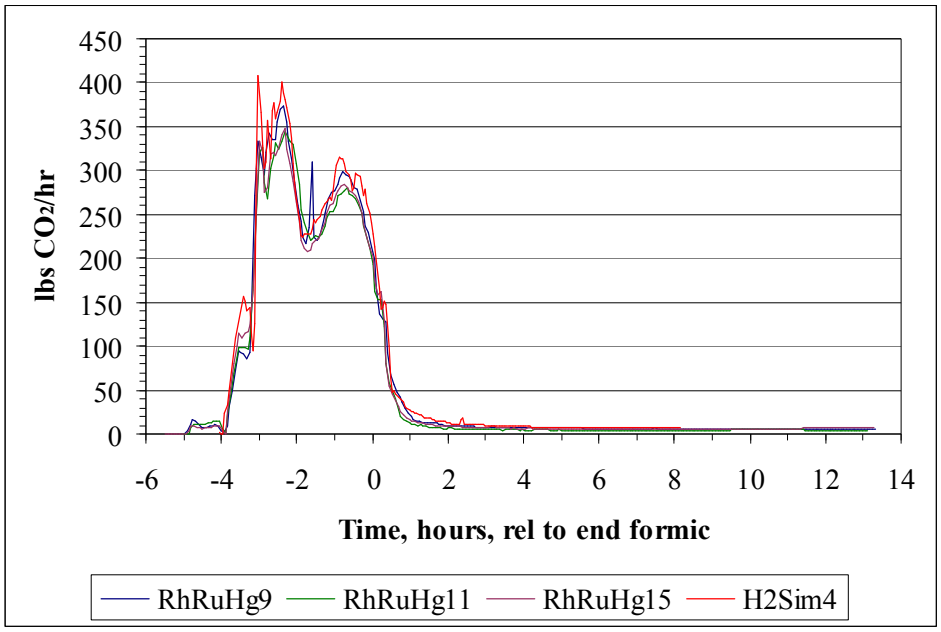

Figure 7. CO_2 generation at midpoint noble metal concentrations

The new data are very similar to the earlier data for CO_2 generation. In particular, the data seem to indicate a nearly identical acid addition was performed on all four tests as planned. Figure 8 gives the corresponding data for N_2O generation.

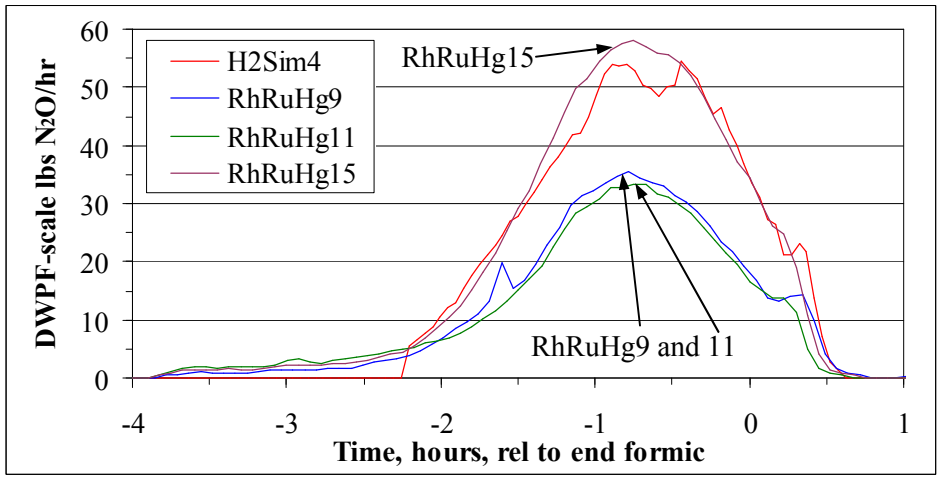

Figure 8. N_2O generation at midpoint noble metal concentrations

Considerable variability is seen in the profiles for N_2O generation. The new midpoint run matches closely with the H2Sim4 data but less well with the two earlier midpoint matrix runs. The four data sets may be demonstrating the likely variability in this measurement over a series of replicate trials rather than indicating anything unusual about any individual test.

4.0 STATISTICAL EVALUATION OF MATRIX DATA

This section summarizes the statistical aspects of the matrix study including the original experimental design, the construction of the hydrogen and process chemistry response variable tables, and the results of statistical modeling of the response variables with the three matrix factors: Rh, Ru, and Hg.

4.1 MATRIX STRUCTURE AND DATA EVALUATION

4.1.1 Matrix Structure and Properties

The experimental matrix constituted a full factorial design on the three factors Rh, Ru, and Hg. Each factor had two primary levels, high and low, as described in Table 1. In addition, there was a midpoint test with each factor at the arithmetic average of its high and low levels. This structure produced the parameter space shown in Figure 9.

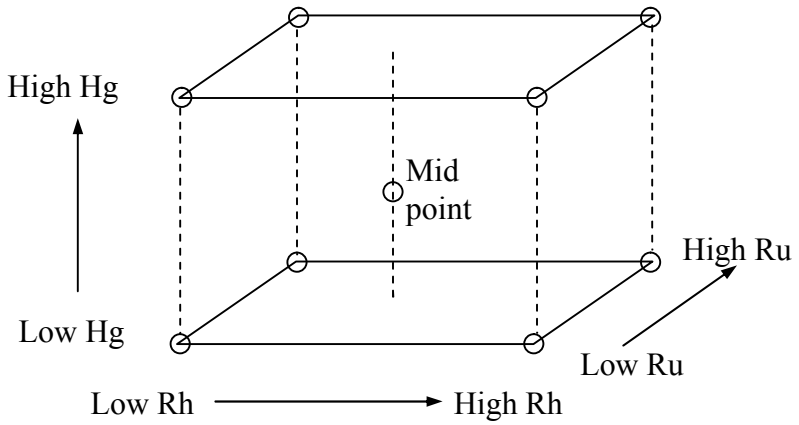

Figure 9. Structure of Rh-Ru-Hg test matrix

Process measures, such as peak hydrogen generation rate, were determined at the design conditions represented by the eight corners of the cube and the midpoint. Averages of a given process measure can be formed at high Hg and low Hg, or at high Rh and low Rh, or at high Ru and low Ru. These process measure averages can be compared to the midpoint value to see if trends are present. Sets of individual process measurement data can be analyzed by statistical software packages to determine the statistical significance of main effects (linear dependence on a first-order factor, either Rh, Ru, or Hg) and to determine the statistical significance of pair-wise interactions of factors (dependence on terms of the form):

$$(Rh - \overline{Rh})(Ru - \overline{Ru}), \quad (Rh - \overline{Rh})(Hg - \overline{Hg}), \quad (Ru - \overline{Ru})(Hg - \overline{Hg})$$

The over-bar denotes the average value of the factor in the test matrix. Interaction terms can change sign as either factor rises or falls. This creates a non-linear effect in the model with respect to the three original factors (low-low and high-high pairs give a positive product, while low-high and high-low pairs give a negative product).

The three binary interaction factors will be abbreviated to Rh*Ru, Rh*Hg, and Ru*Hg in the tables that follow to simplify column headings. The full factorial design ensured that the significance of the three main factors, the three two-factor interactions, and the single three-factor interaction could be evaluated from the testing.

It was possible to test for a general quadratic effect. These appear in the statistical regression model as a quadratic term of one of the three forms:

$$(Rh - \overline{Rh})(Rh - \overline{Rh}), \quad (Hg - \overline{Hg})(Hg - \overline{Hg}), \quad (Ru - \overline{Ru})(Ru - \overline{Ru})$$

These terms do not change sign as the factor changes value from below to above the mean unlike the interaction terms. Testing for a general need of quadratic model terms was possible because the midpoint runs gave a third level for each factor, but the underlying structure of the experimental matrix was not designed to distinguish between the three individual quadratic terms. Consequently, the tables that follow contain a column labeled "Quad" to indicate whether or not a general quadratic dependence was found during modeling.

Six additional SRAT runs centered on the six faces of the test matrix cube would permit identification of specific quadratic effects due to Rh, Ru, and/or Hg. (Few statistically significant quadratic effects were found in the models below, however, so there is little justification for performing the six additional runs.)

4.1.2 Description of the Response Measures

Response measures, such as the maximum hydrogen generation rate during the SRAT cycle, were created from the SRAT processing data in order to evaluate the statistical significance of changes in the three matrix factors on the various responses. Five distinct response measures were created for hydrogen production during the SRAT cycle. These were:

- Total mass of hydrogen produced, g
- SRAT overall maximum (peak) hydrogen generation rate, DWPF-scale lbs/hr
- Maximum hydrogen generation rate in the first two hours after acid addition, lbs/hr
- Maximum hydrogen generation rate in the last four hours of reflux, lbs/hr
- Time of the maximum hydrogen generation rate, in decimal hours

Several additional hydrogen responses were formed by taking the natural logarithm of one of the generation rate responses. The logic for this is as follows. The noble metals and/or mercury are expected to impact the reaction kinetics of hydrogen generation via the catalytic kinetic reaction rate constant(s), since these species are not reactants. These "rate constants" are not true constants, especially when catalysis is involved. If the catalyst controlling hydrogen generation is undergoing a fast or slow exponential loss in activity due to some

parallel reaction process, then a time integration of a general rate expression for hydrogen generation with pseudo-steady state formic acid and/or formate ion concentrations would contain an exponential time function due to the noble metals and/or mercury as well. Taking the logarithm of the reaction rate would reduce the exponential time function to a simpler function of the noble metals and/or mercury that might be more amenable to statistical analysis than the rate itself.

Seven additional response measures of general process chemistry were created for the SRAT cycle based on recent findings related to SRAT chemistry and acid consumption:[12]

- Total CO_2 produced, g (calculated from CO_2/He ratio and Simpson's rule[13])
- % formate destruction (derived from Ion Chromatography, or IC, data and mass balances)
- Total N_2O produced, g (calculated from N_2O/He ratio and Simpson's rule)
- Total NO_2 produced, g (calculated from O_2 consumption)
- Total NO produced, g (estimated using the historical area factor ratios for He and NO)
- Total moles of NO_x in the off-gas (summed from the previous three after conversion)
- % nitrite-to-nitrate conversion (derived from IC data and mass balances)

For calculating the total moles of NO_x, N_2O was treated as $NO_{0.5}$. N_2O_4 cannot be determined separately from NO_2 with the current assumptions and measurements, therefore both gases were lumped together as equivalent NO_2. These two assumptions made the calculation of total moles NO_x equivalent to a sum of moles of nitrogen leaving as gaseous oxides in the off-gas. These moles were presumably derived from an equal number of moles of destroyed nitrite ions (as opposed to nitrate ions).

Two data sets were constructed from sets of the three matrix factors and the twelve response measures. One contained the hydrogen measures and one contained the other process measures. Both data sets contained a full factorial design. Model fitting was performed on the twelve process measures. Fitting considered eight potential model terms. These were Rh, Ru, Hg, the three pair-wise interactions, the single ternary interaction, and a generic quadratic term. The potential three-way interaction term was never justified (models that might have included it contained an excessive number of terms for a database with just twelve points, i.e. they were over fit).

4.2 TESTS OF THE SRAT HYDROGEN MEASURES

4.2.1 Determination of SRAT Hydrogen Measures

The calculated process measures related to hydrogen generation, which were listed in Section 4.1.2, are summarized in Table 2 for the matrix SRAT cycles under consideration.

Table 2. Process Measures for SRAT Hydrogen

	Overall peak H_2, lbs/hr	Total H_2, g	Overall H_2 Peak Time, hr	0-2 hr H_2 peak, lbs/hr	9-13 hr H_2 peak, lbs/hr
Low Mercury Runs					
RhRuHg1	0.0596	0.0199	13.22	0.0180	0.0596
RhRuHg12	0.2330	0.0493	0.47	0.2330	0.0612
RhRuHg10	0.2103	0.0681	7.62	0.0330	0.1785
RhRuHg14	1.415	0.1028	0.53	1.415	0.1459
High Mercury Runs					
RhRuHg5	0.0317	0.0136	13.24	0.0220	0.0317
RhRuHg6	0.1624	0.0239	0.43	0.1624	0.0186
RhRuHg7	0.1793	0.0451	12.54	0.0249	0.1793
RhRuHg8	0.2687	0.1167	12.28	0.2534	0.2687
Midpoint Mercury Runs					
RhRuHg9	0.1118	0.0346	0.87	0.1118	0.0712
RhRuHg11	0.0866	0.0228	0.67	0.0866	0.0448
RhRuHg15	0.1356	0.0375	12.07	0.0730	0.1356
RhRuHg13[§]	0.1552	0.0333	0.60	0.1552	0.0456
RhRuHg4[†]	0.9685	0.1533	0.60	0.9685	0.1486
RhRuHg2[†]	0.2499	0.1231	2.67	0.2155	0.1616

† - these were the two runs with corroded agitator shafts

§ - this was a replicate trial matched to RhRuHg6 conditions

Most of the hydrogen process measures covered a fairly significant range of values relative to the average value of the measure over the entire data set. The Rh-Ru-Hg matrix was designed with the intention of generating fairly wide ranges in the hydrogen measures in order to enhance the visibility of any statistically significant effects in the data. The hydrogen process measures table indicates that a successful design was achieved without having to use unreasonable initial concentrations of Rh, Ru, or Hg.

4.2.2 Modeling of SRAT Hydrogen Measures

The total hydrogen produced during the SRAT cycle will be used to illustrate the general modeling procedure followed for all process measures. The modeling procedure relied on the stepwise regression platform in JMP statistical analysis software (version 5.0.1). Table 3 indicates the terms that appeared in the regression model (75% confidence to enter and 90% to remain) using a capital P for terms with positive coefficients and a capital N for terms with negative coefficients. Dashes indicate terms that were not statistically significant to the model.

Table 3. Model for Total Hydrogen Generated

Rh	Ru	Hg	Rh*Ru	Rh*Hg	Ru*Hg	Quad	R^2	LoF
P	P	N	P	-	-	P	0.95	G

The first three columns indicate whether or not Rh, Ru, or Hg had a statistically significant main effect (in this case all three did). The next three columns indicate whether there were significant interactions between terms (in this case, one between Rh and Ru). The next column indicates if a quadratic effect (non-linear effect due to one or more individual variables) was significant. In this case, there was a significant quadratic, or non-linear, impact on total hydrogen mass. The next to last column gives the R^2 value of the model (recognize that a four term model has five constant coefficients; when there are only 12 results to fit, R^2 tends to be fairly large). Finally, the last column indicates whether or not "lack of fit", or LoF, was indicated (G represents no lack of fit, i.e. good; and L indicates lack of fit). No lack of fit was the desired outcome of the model fitting process.

It is required that when one of the four higher order terms (three interaction terms or the quadratic term) was included in the model, that all of the first-order factors Rh, Ru, and/or Hg included in the higher order term had to be included in the model as well, even if they were not statistically significant in their own right as main factors. Once a model was generated, the factors in the model were tested for correlation. If factors were correlated, then one of the correlated factors was rejected from the model, and a new fit was generated. Generally the first six columns of factors were not correlated due to the full factorial design of the test matrix.

The preferred quadratic factor was Hg^2 for the total hydrogen mass response model. The presence of Hg^2 forced the model to bring in the linear Hg factor, which otherwise would not have been a statistically significant factor at the 90% confidence level. Selecting either Rh^2 or Ru^2 as the quadratic term caused a small reduction in R^2 because both Hg and Hg^2 left the model. Consequently, the primary factors controlling the total mass of hydrogen produced during the SRAT cycle were modeled to be Rh, Ru and their pair-wise interaction along with a possible small contribution from Hg and/or a quadratic effect.

The positive coefficient on the Rh-Ru interaction indicated that the low-low and high-high cases tended to be enhanced in total hydrogen mass while the mixed high-low cases tended to inhibited in total hydrogen. This suggests an optimum Rh/Ru ratio for hydrogen generation exists somewhere in the neighborhood of the fission yield ratio (low-low and high-high cases of Rh-Ru were at the theoretical fission yield ratio).

The statistical model predictions are compared to the twelve total hydrogen mass values in Figure 10, taken from the JMP software.

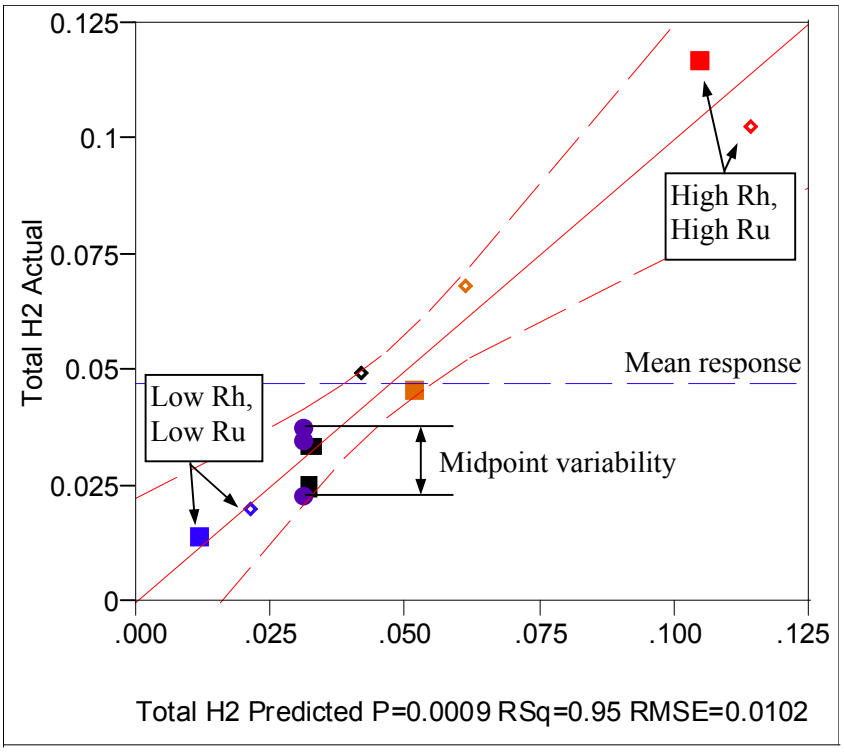

Figure 10. Example comparison of model and data

Data are spread along the model line (45° line) with some small amount of scatter, and with all of the points lying inside the dashed confidence interval curves (no evidence of outliers). The confidence interval dashed lines are a means of graphically showing the significance of the R^2 of the model fit. Note that the variability in reproducing the midpoint case (solid circles) is comparable to the width of the confidence interval curves about the 45° line. The variability due to lack of reproducibility in repeated trials cannot be modeled as a function of the three matrix factors (since they were not changing in value).

Note that this fit is not a general model for predicting hydrogen generation in the SRAT; it is a model for predicting total hydrogen generated for a single sludge with one specific acid stoichiometry over the selected matrix design range of Rh, Ru, and Hg concentrations. Consequently, the numerical values of the individual model coefficients are neither given nor particularly relevant to the conclusions being drawn. Such mathematical model equations would only be useful in predicting hydrogen generation for the same background conditions as in the matrix study, for example the same quantity of excess acid, the same starting nitrite ion concentration, etc.

The same modeling techniques were applied to the overall peak hydrogen generation rates, and the results are given in Table 4.

Table 4. Model for Overall Peak Hydrogen Generation Rate

Rh	Ru	Hg	Rh*Ru	Rh*Hg	Ru*Hg	Quad	R^2	LoF
(P)	P	-	-	-	-	-	0.42	L

JMP initially created a model containing every term (eight constants) during stepwise regression. Eliminating terms not significant at the 90% confidence level after preliminary modeling caused every term but Ru to be eliminated. Rh, however, was significant at the 11% significance level. The near miss was indicated by putting parentheses on P in Table 4. Such near misses were uncommon during modeling. The model also suffered from lack of fit issues. One issue with this data set is that the overall SRAT maximum hydrogen generation rate peaked early in some runs and late in other runs. This model was attempting to explain two apparently different phenomena with a single equation.

The log of the overall peak hydrogen generation rate was fit much better than the linear response. The model included five terms, Rh, Ru, Hg, Rh*Ru, plus a generic quadratic term with an R^2 of 0.92 but still with lack of fit issues. Coefficients for the Rh, Ru, and quadratic terms were positive, while the two coefficients for the Hg and Rh*Ru terms were negative. The noteworthy point is that non-linear terms came into the model.

Based on the results of preliminary modeling of the overall peak hydrogen generation rate, two new responses were created to capture the maximum hydrogen generation rate early and late in the period between the end of acid addition and the end of the SRAT cycle about 13 hours later. The statistical modeling results for the maximum hydrogen generation rate during the first two hours after acid addition are given in Table 5.

Table 5. Models for 0-2 Hour Peak Hydrogen Generation Rate

Rh	Ru	Hg	Rh*Ru	Rh*Hg	Ru*Hg	Quad	R^2	LoF
P	-	-	-	-	-	-	0.25	G

The JMP modeling resulted in a one term model depending on Rh. This model does not explain a large fraction of the variation between cases in the matrix (low R^2). Modeling the log of the early H_2 rate led to a six term model containing Rh, Ru, Hg, Rh*Ru, Rh*Hg, and Ru*Hg with an R^2 of 0.99 and no lack of fit. A seven constant model, however, seems to be excessive for a twelve point data set. Nevertheless, JMP did not include quadratic terms or the third-order interaction in the model of this alternate response of the initial peak rate.

It was anticipated that the hydrogen generation rate maximum in the first two hours after acid addition would show either a main effect or an interaction effect involving mercury. This expectation was based on historical data and a review of the graphs of the Rh-Ru-Hg hydrogen data. A statistically significant Hg effect was only found for the log rate, not the rate itself.

The simple one term model for the linear maximum hydrogen generation rate in the first two hours after acid addition is shown compared to the actual data in Figure 11 for comparison with the high R^2 fit in Figure 10.

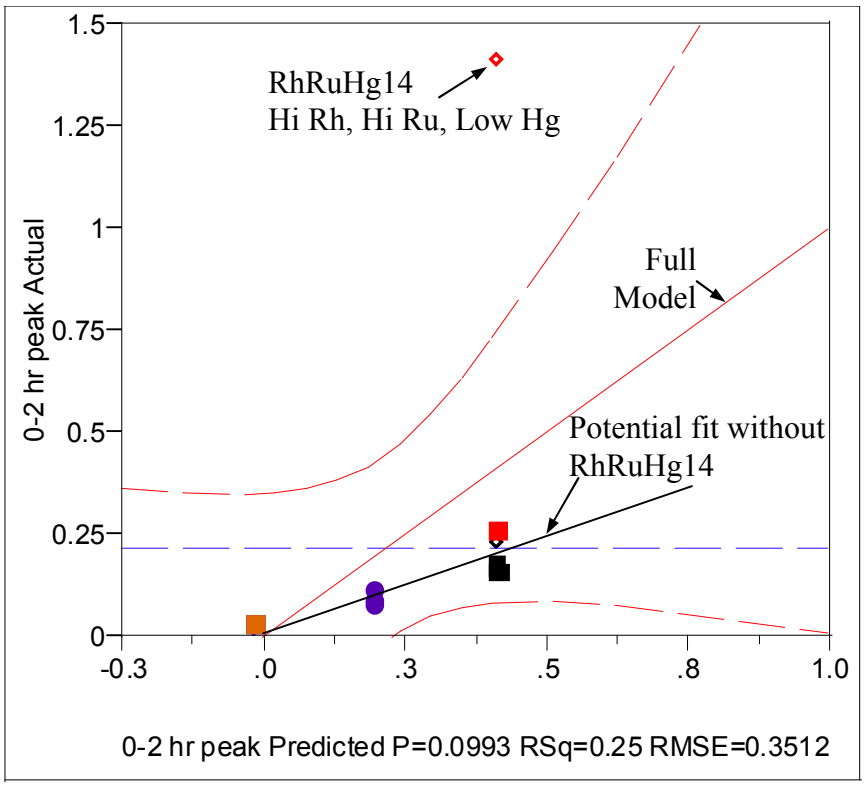

Figure 11. Rh model fit to 0-2 hr H_2 data

Visually, a model based on Rh alone can explain a lot of the variation in the early hydrogen generation rate if the extreme case, RhRuHg14, is rejected (potential fit line with $R^2 \cong 0.87$ ignoring RhRuHg14). Such a model would bring in Hg as a second statistically significant factor. There is no justification, however, for rejecting RhRuHg14 data. Section 3.1 showed that the other RhRuHg14 off-gas data was not unusual. The run it replaced, RhRuHg4, also made significantly more hydrogen than the model. It is more likely that the experimental data indicate some sort of beneficial interaction between Rh and either/both of Ru and Hg to enhance hydrogen generation that could not be picked up by the linear statistical modeling as significant, perhaps because only a single point was involved.

The results for modeling the maximum SRAT hydrogen generation rate in the last four hours of reflux versus the three matrix factors are given in Table 6.

Table 6. Model for 9-13 Hour Peak Hydrogen Generation Rate

Rh	Ru	Hg	Rh*Ru	Rh*Hg	Ru*Hg	Quad	R^2	LoF
-	P	-	-	-	-	-	0.74	G

Another one term model was generated, this time with Ru as the significant factor instead of Rh. Increasing Ru concentration correlated with increasing hydrogen generation rates. The fit was significantly better than that for the 0-2 hour peak generation rate. Modeling the log

of the 9-13 hour rate gave a model containing Ru along with Hg and the Ru*Hg interaction with an R^2 of 0.83 and no lack of fit. This alternative 9-13 hour hydrogen generation rate model showed that mercury had the potential for explaining some of the variation in the hydrogen data not accounted for by the Ru term alone. JMP indicated that Hg was more significant than Rh in explaining variations remaining after including the Ru term. This seems to indicate that Rh was not a major factor 9-13 hours after acid addition for runs that produced some hydrogen shortly after formic acid addition (all of those in the matrix study).

The agreement between the one-term Ru model and measured values is shown in Figure 12.

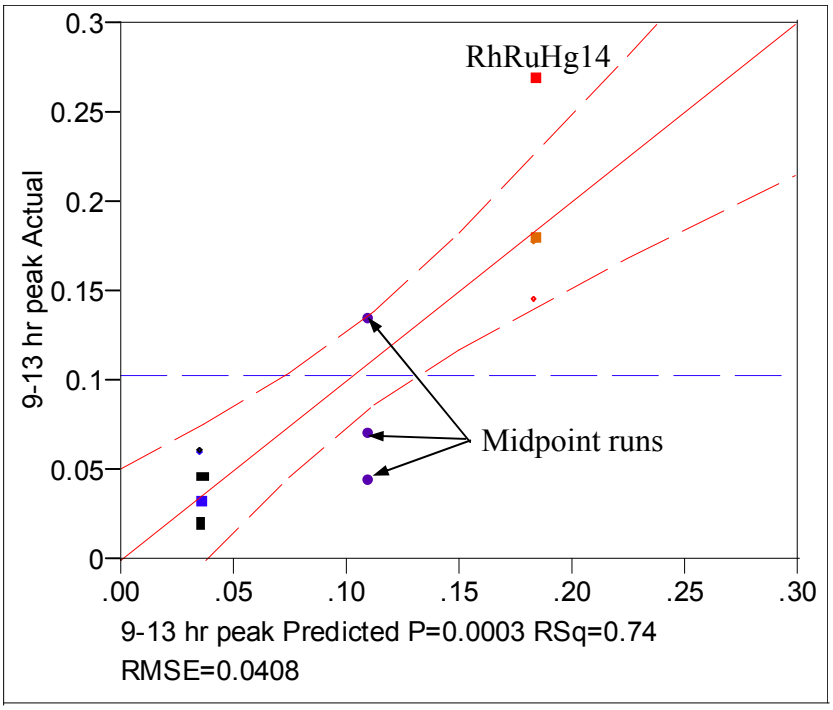

Figure 12. Comparison of model to data for 9-13 hour peak H_2

The variability in hydrogen generation at low and at high Ru concentrations cannot be explained by the one-term Ru model. Two of the points outside the dashed confidence interval traces bracketing the model fit are from two of the midpoint runs. The variability in the three presumably identical (by design) midpoint run responses is significant and explains why more subtle effects may go undetected during the statistical analysis. The third point outside of the dashed confidence interval traces is RhRuHg14, the projected run with maximum catalytic activity due to maximum Rh and Ru combined with minimum Hg.

The fifth measure of SRAT hydrogen generation was fundamentally different from the other four. The first four related to total mass or mass generation rates of hydrogen. The fifth measure was the time that the maximum hydrogen generation rate occurred without regard to the absolute or relative magnitude of the maximum rate itself. The results of modeling the timing of the peak hydrogen generation rate are given in Table 7.

Table 7. Models for Peak Hydrogen Generation Time

Rh	Ru	Hg	Rh*Ru	Rh*Hg	Ru*Hg	Quad	R^2	LoF
N	-	-	-	-	-	-	0.41	G

The model was dominated by Rh. Decreasing Rh concentrations tended to correlate with later peak times. The lack of other terms may again be due to the variability in the timing of the peak in the three midpoint runs, two of which peaked early while the third peaked relatively late.

4.3 TESTS OF THE SRAT CHEMISTRY MEASURES

4.3.1 Determination of SRAT Chemistry Measures

Section 4.3 summarizes the statistical modeling results for the SRAT chemistry response measures listed in Section 4.1.2 with the Rh, Ru, and Hg linear and non-linear terms used in modeling the hydrogen measures. The calculated process chemistry responses for carbon and nitrogen species reactions are summarized in Table 8. Not all of the digits shown may be significant, but the values were used without round-off in statistical modeling work.

Table 8. Process Measures for SRAT Chemistry

	Total CO_2, g	% formate loss	Total N_2O, g	Total NO_2, g	Total NO, g	Total NO_x, moles	% NO_2^- to NO_3^- conv.
RhRuHg1	50.46	11.7	3.42	38.90	2.10	1.071	32.5
RhRuHg12	49.60	16.5	5.04	34.22	0.40	0.986	25.3
RhRuHg10	58.15	11.3	3.40	45.53	1.17	1.183	24.3
RnRuHg14	56.14	18.2	2.34	47.39	0.87	1.165	24.5
RhRuHg5	53.73	11.4	2.70	41.98	1.41	1.082	31.8
RhRuHg6	52.79	9.8	3.62	38.91	0.85	1.039	27.4
RhRuHg7	59.16	14.2	2.62	44.45	0.46	1.100	25.2
RhRuHg8	59.80	21.7	3.25	40.19	2.12	1.092	21.1
RhRuHg9	58.13	14.8	3.02	43.64	3.50	1.202	33.1
RhRuHg11	54.30	18.9	2.87	43.96	0.57	1.105	18.6
RhRuHg15	55.10	16.3	4.95	38.94	1.70	1.128	30.2
RhRuHg13§	55.75	17.5	2.43	41.48	0.64	1.033	21.9
RhRuHg2†	48.97	12.4	4.87	36.97	0.58	1.044	25.5
RhRuHg4†	55.51	11.7	2.95	40.29	4.04	1.144	19.8

† - these were the two runs with corroded agitator shafts

§ - this was a replicate trial matched to RhRuHg6 conditions

The values in the last two rows were not used in preparing the final statistical model equations, as was the case with the models for the hydrogen measures. In general terms, the variations within many of the columns of process measures are not large in magnitude, that is the changing noble metal and mercury concentrations often produced only small percent variations about the mean value of the response. For example, total NO_x moles were at about

1.10 moles ± 10%. When this numerical structure occurs in the data, a simple statistical model based on the average value gives a fairly good estimate for the expected outcome without any terms involving the experimentally varied factors. In this case, the model "total NO_x moles equals 1.10" is fairly good without any additional terms.

4.3.2 Modeling of Measures Containing Carbon

Carbonate, formic acid, formate ion, and CO_2 are the main elements of a carbon-based material balance on the SRAT cycle. Carbon dioxide concentration in the off-gas is measured fairly accurately by the GC, and the conversion to total mass is straight forward using Simpson's rule of numerical integration and the internal He standard flowrate. Two totals of the mass of CO_2 were obtained for each run by off-setting the starting point of the integration by one reading. The two nearly identical totals were averaged (similar methods were used for N_2O, NO_2, and NO). CO_2 should evolve from total inorganic carbon (TIC) destruction and from Hg, Mn, and nitrite reduction reactions with formic acid, as well as from catalytic attack on formic acid and/or formate ion. TIC generated CO_2 should be a constant in all twelve SRAT runs. Table 9 presents the statistical modeling results for total CO_2 mass using JMP.

Table 9. Model for Total CO_2 Production

Rh	Ru	Hg	Rh*Ru	Rh*Hg	Ru*Hg	Quad	R^2	LoF
-	P	P	-	-	N	-	0.86	G

The three term fit with an R^2 of 0.86 was quite good at explaining variation in total CO_2. The Hg term with positive coefficient is presumably related to the increase in CO_2 associated with Hg reduction. The five-fold increase in Hg in the matrix led to a five-fold increase in CO_2 produced during Hg reduction. This increase was large enough to see on plots of the low Hg versus high Hg CO_2 generation rate for each pair of Rh-Ru combinations.[14] Other previously observed Hg effects during nitrite destruction may also be included in this term.[12]

The Ru term seems to indicate that Ru is driving catalytic formate to CO_2 conversion more significantly than Rh in the context of the full SRAT cycle. On average, Ru levels exceeded Rh levels by nearly a factor of four in the matrix. This higher concentration may relate to the selection of Ru over Rh in the model. Data also show considerably more moles of CO_2 than H_2 are generated in the latter stages of the SRAT when catalytic reactions appear to dominate the chemistry and when Ru was the dominant source of hydrogen. The regression result above may also indicate that Ru rather than Rh is controlling catalytic loss of formate unrelated to hydrogen generation, such as catalytic wet air oxidation.

The Ru-Hg interaction term is interesting. That term also appeared when attempting to model the original twelve runs (with the corroded shaft data included). Physically, the term implies that increasing either Ru or Hg while decreasing the other leads to relatively more predicted CO_2 production from this term, while changing both terms in the same direction, either both up or both down, leads to less predicted CO_2 production from this term (although increasing both would lead to more CO_2 production overall due to the other two terms).

Formate loss is associated with CO_2 production. Although no direct statistical model was found to link the two, they were weakly correlated. Modeling formate loss was expected to be more difficult than modeling total CO_2 due to the previously evaluated greater measurement uncertainties. Although percent formate loss was selected for modeling, a model of moles formate loss would have identical information (for the matrix study). The two terms differ only by a multiplicative constant in the matrix study, because all trials received essentially the same formic acid addition (adjusted for variations in initial Hg). Results from formate loss modeling are given in Table 10.

Table 10. Model for Percent Formate Loss

Rh	Ru	Hg	Rh*Ru	Rh*Hg	Ru*Hg	Quad	R^2	LoF
P	P	-	-	-	-	-	0.50	G

The percent formate loss fell roughly in the narrow range 16±6%. This 12% wide range could be considered to be nearly at the noise level for propagated error in calculating the loss, but the statistical modeling result is not unreasonable. Both model coefficients were positive. Increasing Rh or Ru concentration tended to increase formate loss. This is the chemically expected trend for the two catalyst factors: that more catalyst will generally lead to more formate loss. The model for percent formate loss and the one for total CO_2 did have the Ru term in common.

A statistically significant Hg effect may not have shown up in the percent formate loss model (vs. the CO_2 model) because a stoichiometric increase in formic acid was made when Hg was increased in an attempt to provide the same moles of formate ion at the onset of hydrogen generation (which occurred several hours after Hg reduction).

4.3.3 Modeling of Measures Containing Nitrogen

SRAT nitrogen species material balances deal with nitrite, nitrate, and off-gas nitrogen oxides. Ammonium ion is another species that would be covered by a nitrogen species balance. The process measures, that are analyzed below, deal primarily with the chemistry of nitrite destruction. Nitrite destruction is an important component of the stoichiometric acid equation. Its near total destruction often signals the onset of hydrogen generation. Species that change the chemistry of nitrite destruction potentially also change the moles of acid required to consume a mole of nitrite ion. Consequently, analyses of nitrite destruction have been a regular component of recent technical reports. Nitrate destruction and ammonium ion formation can also occur during the SRAT, but these usually occur later in the SRAT cycle and are less significant than nitrite destruction.

Modeling results for total N_2O production did not produce a model equation even though the measure varied from 2.34-5.04 grams per run. The range about the mean value of 3.39 g is more than can be explained by small variations in the He flow controller or GC calibration, that is real variations were observed during the performance of the matrix tests. One potential explanation for the lack of a model is that variations within the replicate trials were large. The midpoint case N_2O data ranged from 2.87-4.95 grams which is not much smaller than the range of the entire matrix data set. One of the two hi-lo-hi runs produced 50% more

N_2O than the other. It is presently unclear as to why there was relatively more variability in the N_2O data than in the CO_2 data which came off the same column of the GC. One hypothesis is that the availability of oxygen may be impacting N_2O formation.

The first bead-frit matching test performed (Ru plus 1.5% Hg) showed that Hg had a large negative impact on the N_2O produced relative to the comparable Ru bead-frit runs with no Hg.[12] This comparison occurred at 0.2 wt% Ru, however, which was considerably more than in the matrix study. The second bead-frit matching test (Rh plus Hg) also showed that Hg had a negative impact on the N_2O produced relative to the pair of comparable runs without Hg (nearly a 40% drop in total N_2O mass with 1.5% Hg added). (This last statement is a preview of a result that has not yet been technically reviewed.) Mercury came closest to entering a linear model for N_2O production of the terms available, but the F-test gave a p-value of 0.297, while a value less than 0.10 was needed.

The total NO_2 produced was calculated from the oxygen loss during nitrite destruction under the assumption that oxygen was lost converting NO to NO_2, and the resulting total automatically includes any NO_2 dimer (N_2O_4) that may have formed. Modeling results for NO_2 production are given in Table 11.

Table 11. Model for Total NO_2 Produced

Rh	Ru	Hg	Rh*Ru	Rh*Hg	Ru*Hg	Quad	R^2	LoF
N	P	P	-	-	N	-	0.77	G

The model showed dependence on all three main factors plus an interaction between Ru and Hg. Tests on preliminary data sets (prior to having the RhRuHg14 and 15 data) also produced models containing Ru-Hg interaction terms in every instance. The positive coefficient for Hg is consistent with other testing that showed that Hg tended to partially suppress N_2O formation (potentially by promoting NO_2 production in its place). The significance of the Rh term was the lowest of those in the model, but the negative coefficient was consistent with previous experimental observations that Rh promotes N_2O formation (at the expense of NO_2 production).

Total NO produced but not converted to NO_2 was estimated from the GC chromatogram areas for the NO peak. The NO peak was only approximately calibrated by using historical data relating the NO area factor to the He area factor for the Agilent 3000A GCs. Consequently, it was probably more uncertain than the total CO_2 or N_2O values. NO, however, was also the least significant of the three NO_x off-gas species in terms of overall molar production. No statistically significant model was found.

The "total moles of nitrogen in the off-gas" was the last off-gas measure tested. It was the sum of the moles of NO plus the moles of NO_2 plus two times the moles of N_2O, that is the sum does not include nitrogen gas. Modeling results for the sum of the off-gas NO_x species are given in Table 12.

Table 12. Model for Total Moles NO_x in Off-gas

Rh	Ru	Hg	Rh*Ru	Rh*Hg	Ru*Hg	Quad	R^2	LoF
N	P	N	-	-	N	N	0.84	G

Ru was the principal factor promoting off-gas NO_x over nitrate ion formation. It appeared in a positive linear term in this and all preliminary models. It was tentatively assigned to the quadratic term in the models, since it was the leading linear term. Rh was a weak negative factor in the model equation. Dropping Rh from the model still produced a good equation with an R^2 of 0.77 and no lack of fit.

The modeling of total moles off-gas NO_x was constrained by the finite quantity of nitrite, and this is discussed further at the end of this sub-section. Total moles of NO_x only varied over a range of about ±10% around the mean. When there was more variation in the response due to the factors (i.e. H_2 and CO_2 responses), the statistical modeling seemed to give more physically sensible results. "Total moles of NO_x in the off-gas" had some off-setting effects from the individual terms in the sum that tended to bring the numbers into a narrow range.

Modeling was also performed on the percent nitrite-to-nitrate conversion measure. As with percent formate loss, this model was equivalent to modeling moles of nitrite converted to nitrate, since all matrix tests nominally started with the same number of moles of nitrite ion. Results are given in Table 13.

Table 13. Model for % Nitrite-to-Nitrate Conversion

Rh	Ru	Hg	Rh*Ru	Rh*Hg	Ru*Hg	Quad	R^2	LoF
N	N	-	-	-	-	-	0.35	G

Rh was the primary factor for nitrite-to-nitrate conversion, followed by Ru. These two factors were also significant in preliminary statistical modeling prior to RhRuHg14 and 15. The model indicates that the two catalysts act to promote nitrogen off-gas species formation at the expense of nitrate formation. The homogeneous nitrite-to-nitrate conversion reaction is a well known reaction requiring no catalysts, so a finding that the presence of catalysts could divert some of the nitrite from converting to nitrate is not inconsistent with other data.

A factor that was difficult to incorporate into the process chemistry response models was the inherent constraint of the starting moles of nitrite ion in the system on the totals of the various by-products of nitrite destruction. Responses like "total moles N in the off-gas" or total NO_2 are constrained by the starting mass of nitrite ion and can only increase so far due to changes in Rh, Ru, and Hg before the system would run out of nitrite ion. The term "Total moles N in the off-gas" accounts for about 70% of the initial nitrite content. The total NO_2 accounts for about 75% of the total off-gas nitrogen oxides. Neither of these responses can increase much further before taking on physically impossible values.

The statistical models derived to explain the observed variations using linear terms in the concentrations of the three factors only indicate trends over the range of Rh, Ru, and Hg values used in the matrix design (interpolation), but it is clear that they quickly become

invalid outside of that range (extrapolation) when looking at nitrite destruction. Higher order (nonlinear) terms would have to be present in a theoretical model describing the response to mercury and noble metal concentrations in order to avoid predicting physically unrealistic outcomes as concentrations increase above those in the matrix study.

An alternative way of looking at the NO_x and nitrite-to-nitrate conversion responses is to test them for correlation with each other. Correlation is expected since as one or more of the responses go up, the remaining responses derived from nitrite destruction must go down to compensate. The simplest test is to look at correlation between N_2O, $NO+NO_2$, and nitrite-to-nitrate conversion. NO was lumped with NO_2 since the NO_2 is derived from nitrite converted to NO which reacts with oxygen to form NO_2 (or N_2O_4).

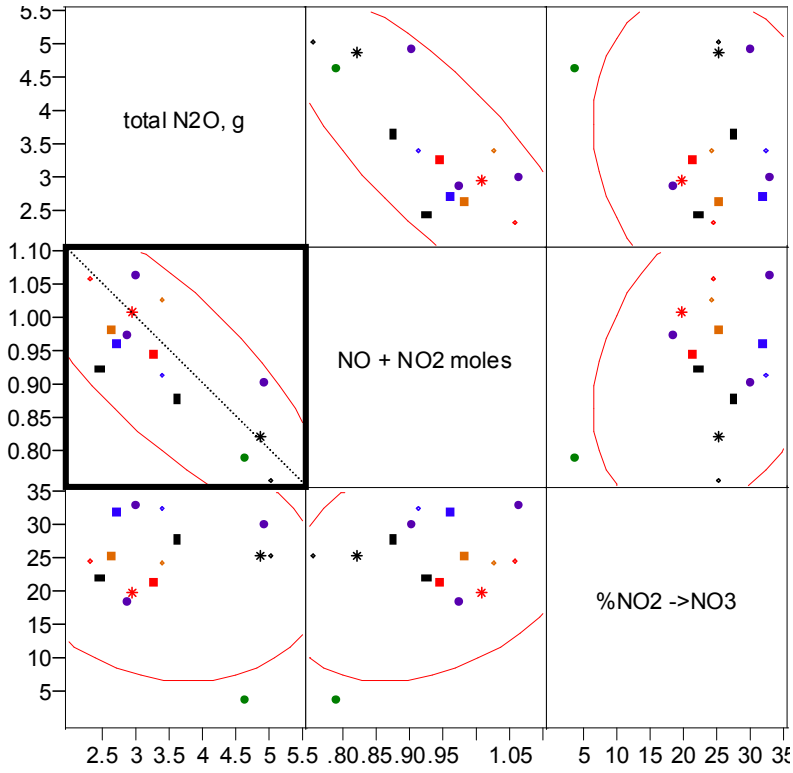

Figure 13. Test for correlation among nitrite by-products

A strong negative correlation was found between the NO-derived off-gases and the N_2O off-gas (correlation of -0.791, with a perfect negative correlation indicated by a -1.00 result). The relevant panel is high-lighted with a bold border in the figure. Although a statistically significant model was not found for N_2O in terms of Rh, Ru, and Hg and their interactions, the scatterplot matrix results indicate that, at least in broad terms, factors tending to increase NO and NO_2 production tended to decrease N_2O production. Conversely, nitrite-to-nitrate conversion appeared to be relatively insensitive to changes in the distribution of the off-gas species (it is also possible that the relatively higher uncertainty, or scatter, in the calculated nitrite-to-nitrate conversion percentages compared to the GC-derived off-gas moles was responsible for the apparent lack of correlation).

There was general lack of correlation between the nitrogen off-gas species and the percent nitrite-to-nitrate conversion response, even though all were derived from the fixed quantity of available nitrite ion in the starting sludge. This lack of correlation puts the accuracy of the nitrite-to-nitrate conversion data into question, and consequently the correlation in Table 13 may be the result of a serendipitous alignment of random effects rather than a true correlation. The favored interpretation is that the two effects in Table 13 are real, since they were seen in multiple permutations of the available matrix run data, they did not seem to explain an unreasonably high fraction of the variation in the nitrite-to-nitrate conversion responses, and they were not inconsistent with data from the bead-frit tests with this same starting simulant.

Actual acid consumption in the SRAT cycle is increased by promoting the formation of N_2O and/or the catalytic reduction of nitrite to NO by formic acid. These two reactions require 2.0 and 1.5 moles of acid per mole of nitrite, respectively, compared to two-thirds of a mole of acid per mole of nitrite for the nitrite-to-nitrate conversion reaction. The net acid consumed by nitrite is the weighted average of these three reactions. This picture is further complicated by potential internal refluxing of nitrous acid on the equipment walls. The theoretical range is 0.67-2.0 moles of acid per mole of nitrite for an ideal system (no internal refluxing), and much recent data have fallen in the vicinity of 1.0-1.1 moles of acid per mole of nitrite destroyed when modeled as ideal.

It appears that two factors have helped to keep recent results for acid consumption due to nitrite ion destruction in a relatively narrow range. First, nitrite-to-nitrate conversion has not been varying that much. The fraction of nitrite destroyed at a cost of 0.67 moles acid per mole nitrite into one mole of nitrate plus two moles of NO gas was fairly steady at 27±7%. (This is 81±21% of the nitrite.) Second, the competition between N_2O and NO formation reactions (seen in the negative correlation results) is not producing a significant shift in acid consumption. For example, if the fraction of nitrite converted to nitrate is constant, and the relative distribution of N_2O to all NO derived off-gases (NO, NO_2, N_2O_4, but excluding those from nitrite-to-nitrate conversion) shifts from 20:80 to 80:20, then the acid consumption for the nitrite not undergoing the nitrite-to-nitrate conversion reaction shifts from 1.6 to 1.9 moles acid per mole nitrite. (This shift only applies to the nitrite not converting to nitrate plus two NO molecules, or typically to about 20-40% of the total nitrite.) The overall impact on acid required to destroy nitrite is considerably less than the 0.3 moles acid per mole nitrite shift caused by redistributing the remaining off-gas species from 20:80 to 80:20, and probably produces less than a 0.1 moles acid/mole nitrite swing in overall acid consumption for typical noble metal and mercury concentration ranges.

5.0 CONCLUSIONS

An evaluation of the statistical significance of Rh, Ru, and Hg on DWPF SRAT cycle hydrogen generation and process chemistry was conducted using a full-factorial experimental design. The test matrix was designed to detect significant interactions between these three species. Statistical modeling of data from the Rh-Ru-Hg matrix study was completed. Preliminary data and conclusions were given in an earlier report.[10] This report concludes the work on the Rh-Ru-Hg matrix study. Modeling results are summarized below.

Rhodium by itself was found to:

- Promote increased total hydrogen mass.
- Promote an increase in the maximum hydrogen generation rate.
- Promote an increase in the hydrogen generation rate shortly after acid addition.
- Shorten the elapsed time between acid addition and the maximum hydrogen generation rate.
- Increase formate loss.
- Inhibit NO_2 and total NO_x off-gas species formation.
- Reduce nitrite-to-nitrate conversion.

Ruthenium was found to:

- Promote increased total hydrogen mass.
- Promote an increase in the maximum hydrogen generation rate.
- Promote an increase in the hydrogen generation rate in the second half of the SRAT cycle.
- Promote an increase in total CO_2 generated.
- Increase formate loss.
- Promote NO_2 and total NO_x off-gas species formation.
- Reduce nitrite-to-nitrate conversion.

Mercury overall was found to:

- Inhibit total hydrogen mass produced.
- Promote an increase in total CO_2 generated.
- Promote NO_2 off-gas species formation.
- Inhibit total NO_x off-gas species formation.

Results confirmed qualitative observations that Rh was activating before Ru for hydrogen generation. An interaction between Rh and Ru was present in the model for the total hydrogen generated during the SRAT, perhaps because this total included contributions from two separate episodes of hydrogen generation the first of which was dominated by Rh and the second by Ru, that is the model was forced to explain more than one phenomenon.

Mercury did not significantly impact hydrogen generated by either Rh or Ru in linear models in this study (all tests included at least 0.5 wt% mercury in the total solids), whereas tests in SB3 and SB4 with and without Hg showed a very significant negative impact from adding Hg. The conclusion is that once a small quantity of Hg is present, the primary inhibiting effect of Hg is in place, and hydrogen generation is relatively insensitive to further increases in total Hg (any secondary Hg effects were difficult to quantify, and, if present, hard to model). Mercury was statistically significant as an inhibiting factor for hydrogen generation when modeling was based on the logarithm of the hydrogen generation rate.

There was only limited statistical evidence for non-linearity and quadratic dependence of the other SRAT process measures on the three matrix variables. The interaction term for Ru with Hg, however, appeared in models for total CO_2, total NO_2, and total moles of nitrogen off-gas species. A single interaction between Ru and Hg during nitrite destruction could explain all three of these effects in the observed responses. Catalytic decomposition of nitrite ion by formic acid can produce NO plus CO_2. The vast majority of the NO produced is converted to NO_2, and NO_2 is the major fraction of the total moles of nitrogen in the off-gas species.

6.0 FUTURE WORK

The completion of the Rh-Ru-Hg matrix study and the bead-frit melter feed preparation campaign (summarized in four technical reports), along with several smaller connected projects that were documented in inter-office memos, has produced a considerable quantity of interrelated new data related to hydrogen generation, noble metal chemistry, and acid consumption (or the determination of excess acid for hydrogen).

Support for various hypotheses concerning the active catalyst noble metal and for its speciation have been obtained. A clearer understanding of what conditions enable hydrogen generation has been developed. SRAT samples containing Rh with and without Hg are awaiting analysis by X-ray spectroscopy in mid-2009 to support some of the hypotheses concerning oxidation state of Rh and significance of Hg to Rh catalysis. This is an appropriate time to take a step back and start to bring all of this information together into a comprehensive summary. The current plan calls for this assessment process to begin following completion of this technical report. The plan calls for generating a summary document on the overall advances made in the understanding of hydrogen generation during the past few years.

Simultaneously with this effort, a new focus has been put on replacing as much of the formic acid as possible with an alternative acid/reductant, for example, glycolic acid. Larger scale tests are planned to evaluate the potential for hydrogen generation and to better quantify any issues with mercury reduction. Another effort has led to some promising results with mesoporous silica supported ligands that can sequester the Rh and Ru and prevent them from becoming catalytically active. Tests at ~30 g scale have been completed showing dramatic reductions in total off-gas generation, but these measurements have not identified which gases were reduced in total mass or by how much.

The catalytic hydrogen generation program itself needs to reevaluate historical data and issues raised in past review reports in light of the new information that has been obtained. It is believed that a high percentage of those issues have either been resolved or at least better bounded by the new information. These advances need to be documented for the record.

7.0 REFERENCES

[1] Plodinec, M. J., *Report of the Hydrogen Generation Review Panel – Review of Hydrogen Generation in the DWPF*. March 15, 2007.

[2] HLW-DWPF-TTR-2007-0016, Catalytic Hydrogen Generation Program, B. A. Davis, March 8, 2007.

[3] Koopman, D. C., *Task Technical and Quality Assurance Plan – Catalytic Hydrogen Generation Program.* WSRC-RP-2007-00338, SRNL, Aiken, SC, 29808 (April 2007).

[4] Koopman, D. C., *Analytical Study Plan for Catalytic Hydrogen Generation Program.* SRNL-PSE-2007-00154, SRNL, Aiken, SC, 29808 (August 2007).

[5] Koopman, D. C. and M. A. Baich, *Effect of Mercury-Noble Metal Interactions on SRAT Processing of SB3 Simulants*. WSRC-TR-2004-00548, Savannah River Site, Aiken, SC, 29808 (December 2004).

[6] Koopman, D. C., *DWPF Hydrogen Generation Study – Form of Noble Metal SRAT Testing*. WSRC-TR-2005-00286, Savannah River Site, Aiken, SC, 29808 (July 2005).

[7] Koopman, D. C., *DWPF Hydrogen Generation Study: Phase II – Form of Noble Metal SRAT Testing*. WSRC-TR-2005-00420, SRNL, Aiken, SC 29808 (December 2005).

[8] Baich, M. A., C. C. Herman, D. R. Best, M. F. Williams, and E. K. Hansen, *Sludge Batch 4 Initial Simulant Flowsheet Studies: Phase I SRAT Results*, WSRC-TR-2005-00194, SRNL, Aiken, SC 29808 (June 2005).

[9] Koopman, D. C., *Preparation, Characterization, and Preliminary SRAT/SME Testing of a Simulant for the Hydrogen and Rheology Modifiers Program.* SRNL-PSE-2007-00191, SRNL, Aiken, SC, 29808 (September 2007).

[10] Koopman, D. C., *Catalytic Interactions of Rhodium, Ruthenium, and Mercury during Simulated DWPF CPC Processing with Hydrogen Generation*, WSRC-STI-2008-00235. SRNL, Aiken, SC, 29808 (July 2008).

[11] Koopman, D. C., T. B. Edwards, and M. D. Joner, *Summary of Findings Based on Statistical Analysis of a SRAT-SME Database*. SRNL-PSE-2007-00207, SRNL, Aiken, SC, 29808 (October 2007).

[12] Koopman, D. C., D. R. Best, and B. R. Pickenheim, *SRAT Chemistry and Acid Consumption During Simulated DWPF Melter Feed Preparation*, WSRC-STI-2008-00131, SRNL, Aiken, SC, 29808 (December 2008).

[13] CRC Standard Mathematical Tables, 23rd Edition, S, M. Shelby, Editor-in-chief, 1975, CRC Press, pg. 14.

[14] Koopman, D. C., *Timing of Mercury Reduction During SRAT Acid Addition*, SRNL-PSE-2008-00169, SRNL, Aiken, SC, 29808 (August 2008).

Distribution:

J. C. Griffin, 773-A
S. L. Marra, 773-A
C. C. Herman, 999-W
A. B. Barnes, 999-W
D. A. Crowley, 773-43A
S. D. Fink, 773-A
C. W. Gardner, 773-A
B. J. Giddings, 786-5A
F. M. Pennebaker, 773-42A

J. E. Occhipinti, 704-S
E. W. Holtzscheiter, 704-15S
T. L. Fellinger, 704-26S
J. M. Bricker, 704-27S
R. T. McNew, 704-27S
D. C. Sherburne, 704-S
J. F. Iaukea, 704-30S
J. W. Ray, 704-S
H. H. Elder, 704-24S
M. C. Clark, 704-27S
D. J. McCabe, 773-42A
C. J. Bannochie, 773-42A
D. K. Peeler, 999-W
N. E. Bibler, 773-A
R. E. Eibling, 999-W
M. E. Stone, 999-W
D. P. Lambert, 999-W
B. R. Pickenheim, 999-W
A. I. Fernandez, 999-W
J. D. Newell, 999-W
J. M. Pareizs, 773-A
S. H. Reboul, 773-42A
C. J. Bannochie, 773-42A
M. F. Williams, 999-W